REPORT DOCUMENTATION PAGE

Form Approved
OMB No. 0704-0188

1. AGENCY USE ONLY (Leave blank)	2. REPORT DATE	3. REPORT TYPE AND DATES COVERED
		Reprint

4. TITLE AND SUBTITLE

Title shown on Reprint

5. FUNDING NUMBERS

ARO MIPR 120-90

6. AUTHOR(S)

Authors listed on Reprint

7. PERFORMING ORGANIZATION NAME(S) AND ADDRESS(ES)

National Institute of Standards & Technology
Gaithersburg, Maryland 20899

8. PERFORMING ORGANIZATION REPORT NUMBER

9. SPONSORING / MONITORING AGENCY NAME(S) AND ADDRESS(ES)

U. S. Army Research Office
P. O. Box 12211
Research Triangle Park, NC 27709-2211

10. SPONSORING / MONITORING AGENCY REPORT NUMBER

ARO 25664.9-CH

11. SUPPLEMENTARY NOTES

The view, opinions and/or findings contained in this report are those of the author(s) and should not be construed as an official Department of the Army position, policy, or decision, unless so designated by other documentation.

12a. DISTRIBUTION / AVAILABILITY STATEMENT

Approved for public release; distribution unlimited.

12b. DISTRIBUTION CODE

13. ABSTRACT (Maximum 200 words)

ABSTRACT SHOWN ON REPRINT

A-1 20

14. SUBJECT TERMS			15. NUMBER OF PAGES
			16. PRICE CODE
17. SECURITY CLASSIFICATION OF REPORT	18. SECURITY CLASSIFICATION OF THIS PAGE	19. SECURITY CLASSIFICATION OF ABSTRACT	20. LIMITATION OF ABSTRACT
UNCLASSIFIED	UNCLASSIFIED	UNCLASSIFIED	UL

Published in Journal of Physical Chemistry, April 4, 1991, 2781-3787, by the American Chemical Society

Vibrational Spectra of Molecular Ions Isolated in Solid Neon. 6. CO_4^-

Marilyn E. Jacox*

Molecular Physics Division, National Institute of Standards and Technology, Gaithersburg, Maryland 20899

and Warren E. Thompson†

National Science Foundation, Washington, D.C. 20550 *(Received: September 26, 1990)*

When a Ne:CO_2:O_2 = 200:1:1 mixture is codeposited at approximately 5 K with a beam of neon atoms that have been excited in a microwave discharge, several prominent infrared absorptions appear in the resulting deposit. In addition to the absorptions of unreacted CO_2, absorptions previously assigned to O_4^+ and O_4^- are present, and new absorptions appear at 697, 1256, 1865, and 1895 cm^{-1}. Detailed isotopic substitution experiments demonstrate that these new absorptions are contributed by a product of formula CO_4 in which the CO_2 moiety is joined to O_2 in such a way that the two O atoms of each of these groups are nonequivalent. Arguments are presented indicating that this product is the CO_4^- anion. The infrared frequencies of the isotopically substituted species have been used for a least-squares force constant adjustment calculation, assuming a planar $O_2C\cdots O_2^-$ (C_s) structure in which most of the negative charge remains on the O_2 moiety. The photodestruction threshold of CO_4^- lies near 260 nm. Evidence has been obtained for the formation of CO_3^- or of CO_3 in an excited state with 3-fold symmetry, for which randomization of the oxygen isotopic substitution occurs.

Introduction

Early in the study of dimer ions, the products of the reaction of CO_2 with O_2^+ and O_2^- were found to have surprisingly large binding energies. Conway[1] first obtained mass spectrometric evidence for CO_4^- in a study of the attachment of low-energy electrons to mixtures of O_2 and CO_2 and proposed a T-shaped structure, resulting from the attack of O_2^- on the carbon atom of CO_2. Drift tube measurements by Pack and Phelps[2] determined that CO_4^- is stable by 18.4 kcal/mol with respect to $O_2^- + CO_2$. Moruzzi and Phelps[3] obtained the rate constant of the three-body reaction by which CO_4^- is formed. Temperature-controlled flowing afterglow studies in the laboratory of Ferguson[4] explored this system with helium as a third body and determined that at 200 K the three-body reaction of O_2^+ with CO_2 to form CO_4^+ also occurs rapidly, although at a rate only half as great as that for the formation of CO_4^-. In addition to providing evidence for CO_4^+, the measurements from that study led to revision[5] of the dissociation energy of CO_4^- to 21 kcal/mol. Recent experiments[6-8] have determined a binding energy of 9.8 kcal/mol for CO_4^+.

The ubiquity of CO_2 and O_2 and the comparatively great stability of CO_4^- suggest that this species may be important in the chemistry of high-energy systems. In 1969, a flowing afterglow study by Fehsenfeld and co-workers[9] determined that CO_2 reacts readily with O_4^- to form CO_4^-. In turn, CO_4^- was found to react with NO and with O atoms, suggesting that it may participate in the chemistry of the upper atmosphere and lower ionosphere. Rocket flights through the D region of the ionosphere with negative ion detection[10,11] measured a signal at mass 76, appropriate for CO_4^- and/or SiO_3^-. Subsequent reaction rate studies[12-15] provided supporting evidence for the role of CO_4^- in ionospheric chemistry, and it is generally included in models of the chemistry of the D region, exemplified by those of Wisemberg and Kockarts[16] and of Thomas and Bowman.[17] Calculations by Shields and Smith[18] also indicate that CO_4^- may be one of the principal anion species that contribute to plasma instability in low-pressure electric discharge convection CO_2 lasers.

Despite these observations of CO_4^- in chemical reaction systems, little is known about its structure or molecular energy levels. Several workers[19-21] have reported the electron spin resonance (ESR) spectrum of CO_4^- on surfaces maintained at 77 K. These studies indicate that most of the electron spin density is concentrated on the two O atoms of the O_2 moiety and that these two O atoms are nonequivalent. Vestal and Mauclaire[22] found only small ion yields in their study of the photodissociation of CO_4^- at six wavelengths between 600 and 305 nm. More detailed gas-phase studies by Moseley and co-workers,[23-25] again using mass spectrometric detection, failed to reproduce the fragment ion signal at 365 nm reported by Vestal and Mauclaire and concluded that the photodestruction cross section of CO_4^- is small over the entire 840–350-nm range.

Recent experiments in this laboratory have used neon atoms in their lowest excited states (16.6–16.8 eV) as a photoionization and Penning ionization source for the production of small molecular ions, which are trapped in a neon matrix at approximately 5 K. The test molecule chosen for the first study[26] was CO_2, which has a first ionization potential of 13.8 eV. Both CO_2^+ and CO_2^- were detected, demonstrating that this sampling technique, previously used by Knight and co-workers[27,28] for more sensitive ESR

† Guest Researcher at the National Institute of Standards and Technology.

(1) Conway, D. C. *J. Chem. Phys.* **1962**, *36*, 2549.
(2) Pack, J. L.; Phelps, A. V. *J. Chem. Phys.* **1966**, *45*, 4316.
(3) Moruzzi, J. L.; Phelps, A. V. *J. Chem. Phys.* **1966**, *45*, 4617.
(4) Adams, N. G.; Bohme, D. K.; Dunkin, D. B.; Fehsenfeld, F. C.; Ferguson, E. E. *J. Chem. Phys.* **1970**, *52*, 3133.
(5) Fehsenfeld, F. C.; Albritton, D. L.; Streit, G. E.; Davidson, J. A.; Howard, C. J.; Ferguson, E. E. *Atmos. Environ.* **1977**, *11*, 283.
(6) Kim, H.-S.; Kuo, C.-H.; Bowers, M. T. *J. Chem. Phys.* **1987**, *87*, 2667.
(7) Hiraoka, K.; Nakajima, G.; Shoda, S. *Chem. Phys. Lett.* **1988**, *146*, 535.
(8) Illies, A. J. *J. Phys. Chem.* **1988**, *92*, 2889.
(9) Fehsenfeld, F. C.; Ferguson, E. E.; Bohme, D. K. *Planet. Space Sci.* **1969**, *17*, 1759.
(10) Narcisi, R. S.; Bailey, A. D.; Della Lucca, L.; Sherman, C.; Thomas, D. M. *J. Atmos. Terr. Phys.* **1971**, *33*, 1147.
(11) Arnold, F.; Viggiano, A. A.; Ferguson, E. E. *Plant. Space Sci.* **1982**, *30*, 1307.
(12) Fehsenfeld, F. C.; Ferguson, E. E. *J. Chem. Phys.* **1974**, *61*, 3181.
(13) Fehsenfeld, F. C. *J. Chem. Phys.* **1975**, *63*, 1686.
(14) Dotan, I.; Albritton, D. L.; Fehsenfeld, F. C.; Streit, G. E.; Ferguson, E. E. *J. Chem. Phys.* **1978**, *68*, 5414.
(15) Viggiano, A. A.; Morris, R. A.; Paulson, J. F. *J. Chem. Phys.* **1989**, *91*, 5855.
(16) Wisemberg, J.; Kockarts, G. *J. Geophys. Res.* **1980**, *85*, 4642.
(17) Thomas, L.; Bowman, M. R. *J. Atmos. Terr. Phys.* **1985**, *47*, 547.
(18) Shields, H.; Smith, A. L. S. *Appl. Phys.* **1978**, *16*, 111.
(19) Ben Taarit, Y.; Vedrine, J. C.; Naccache, C.; de Montgolfier, Ph.; Meriaudeau, P. *J. Chem. Phys.* **1977**, *67*, 2880.
(20) Lipatkina, N. I.; Shubin, V. E.; Shvets, V. A.; Chuvylkin, N. D.; Kazanskii, V. B. *Kinet. Katal.* **1982**, *23*, 670; *Kinet. Catal. (Engl. Transl.)* **1982**, *23*, 565.
(21) Gonzalez-Elipe, A. R.; Louis, C.; Che, M. *J. Chem. Soc., Faraday Trans. 1* **1982**, *78*, 1297.
(22) Vestal, M. L.; Mauclaire, G. H. *J. Chem. Phys.* **1977**, *67*, 3758.
(23) Smith, G. P.; Lee, L. C.; Cosby, P. C.; Peterson, J. R.; Moseley, J. T. *J. Chem. Phys.* **1978**, *68*, 3818.
(24) Cosby, P. C.; Ling, J. H.; Peterson, J. R.; Moseley, J. T. *J. Chem. Phys.* **1978**, *69*, 5267.
(25) Smith, G. P.; Lee, L. C.; Moseley, J. T. *J. Chem. Phys.* **1979**, *71*, 4034.
(26) Jacox, M. E.; Thompson, W. E. *J. Chem. Phys.* **1989**, *91*, 1410.

studies, would also permit detection of the infrared spectra of molecular ions. In some of the experiments on CO_2 samples, other absorptions were also present. Two of these, at 1164 and 1320 cm^{-1}, were subsequently assigned[29] to O_4^+, which resulted from O_2 introduced through a small leak in the Ne:CO_2 system. Two other absorptions, at 1256 and 1895 cm^{-1}, were present in some of the Ne:CO_2 experiments but not in the Ne:O_2 experiments. The demonstration that dimer ions such as O_4^+ could be stabilized under the sampling conditions of these experiments and the relatively large binding energies of CO_4^+ and CO_4^- suggested the study of Ne:CO_2:O_2 samples. This paper reports the results of experiments on that system.

Experimental Details[30]

The carbon dioxide, oxygen, and neon samples used for these experiments were the same as those used for the earlier experiments,[26,29] except that samples of CO_2 randomly enriched to 50% in oxygen-18 (Cambridge Isotope Laboratories, Inc.) and to 97% in oxygen-18 (Merck, Sharp, and Dohme Canada Ltd.) were available. Ne:CO_2:O_2 samples of mole ratio 200:1:1 were prepared by using standard manometric procedures.

The Ne:CO_2:O_2 sample was codeposited at approximately 5 K with a sample of pure neon that had been passed through a microwave discharge. Details of the discharge sampling configuration have previously been described.[26] In order to minimize the access of visible and ultraviolet radiation to the sample, the exterior of the pinhole end of the quartz discharge tube was coated with platinum. Microwave power was coupled to the pure neon in the discharge tube by using a coaxial stub stretcher tuner and a termination fixture of the design developed by Haugsjaa.[31] A Helitran (APD Cryogenics, Inc.) continuous transfer liquid helium cell was used for the experiments.

Absorption spectra of the resulting deposits were studied in the 600–4000-cm^{-1} spectral region by using a Bomem DA3.002 Fourier transform interferometer with a globar source, a KBr beam splitter, transfer optics which have previously been described,[32] and a HgCdTe detector cooled to 77 K. In all of the experiments, at least 128 scans, taken at a resolution of 0.2 cm^{-1}, were coadded. The resulting spectrum was ratioed against a similar spectrum taken without a sample deposit on the cryogenic mirror. In order to obtain further information regarding electron photodetachment and molecular photodissociation processes in the matrix sample, after the infrared spectrum of the initial deposit had been recorded the sample was subjected to the full or filtered output of a medium-pressure mercury arc. Corning filters of glass types 3384, 3389, 7380, 0160, 7740, and 7058 were used to provide radiation with short-wavelength cutoffs near 490, 420, 345, 300, 280, and 260 nm, respectively.

Observations

In all of the studies of Ne:CO_2:O_2 samples, prominent absorptions assigned to O_4^+ and O_4^- in the Ne:O_2 study[29] were present, as were a weak to moderately intense absorption at 796.3 cm^{-1}, assigned[33,34] to O_3^-, and a moderately intense absorption of O_3 near 1040 cm^{-1}. Absorptions previously assigned[26] to CO_2^+ and CO_2^- usually were not detected. In most of the experiments, very small atmospheric leaks in the discharge system resulted in the appearance of absorptions of NO, N_2O, and NO_2, as well as of NO_2^-[35] and sometimes of N_2O_3.[36] A very sharp, structured, weak to moderately intense absorption at 2045.1 cm^{-1} corresponded closely in frequency to the strongest absorption reported[37] for neutral CO_3 isolated in a CO_2 matrix. Prominent, previously unidentified absorptions also appeared at 697.1, 1256.5, 1865.1, and 1895.2 cm^{-1}. The spectral regions of these absorptions are shown in traces a of Figure 1. Weaker absorptions appeared at 1009, 1430, 1436, 2249, and 3255 cm^{-1}.

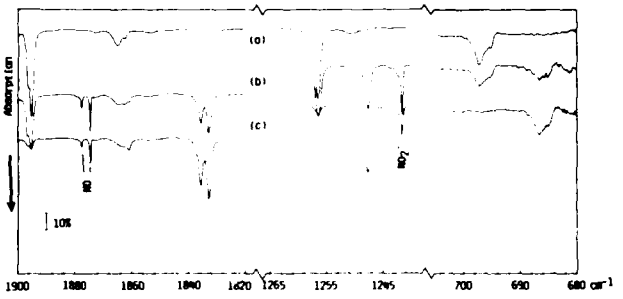

Figure 1. (a) 6.53 mmol of Ne:CO_2:O_2 = 200:1:1 codeposited over period of 134 min with 6.27 mmol of discharged Ne. (b) 6.53 mmol of Ne:CO_2 (51.6% ^{13}C):O_2 = 200:1:1 codeposited over period of 214 min with 8.45 mmol of discharged Ne. (c) 6.53 mmol of Ne:CO_2 (90% ^{13}C):O_2 = 200:1:1 codeposited over period of 129 min with 6.63 mmol of discharged Ne.

TABLE I: Absorptions[a] (cm^{-1}) with a Photodestruction Threshold near 260 nm Observed for Ne:CO_2:O_2 = 200:1:1 Samples Prepared with Normal and Carbon-13-Enriched CO_2 and Codeposited at 5 K with a Beam of Excited Neon Atoms

$^{12}C^{16}O_2 + {}^{16}O_2$	$^{13}C^{16}O_2$ (51.6%) + $^{16}O_2$	$^{13}C^{16}O_2$ (90%) + $^{16}O_2$	assignment
	686.5 wm	686.4 m	$^{16}O_2{}^{13}C\cdot\cdot{}^{16}O_2^-$
695.2 sh			$^{16}O_2{}^{12}C\cdot\cdot{}^{16}O_2^-$
697.1 m	697.1 wm		$^{16}O_2{}^{12}C\cdot\cdot{}^{16}O_2^-$
	1247.6 ms	1247.6 s	$^{16}O_2{}^{13}C\cdot\cdot{}^{16}O_2^-$
1256.5 s	1256.4 ms	1256.5 wm	$^{16}O_2{}^{12}C\cdot\cdot{}^{16}O_2^-$
	1832.7 ms	1832.8 s	$^{16}O_2{}^{13}C\cdot\cdot{}^{16}O_2^-$
	1835.6 m	1835.6 ms	$^{16}O_2{}^{13}C\cdot\cdot{}^{16}O_2^-$
		1861.0 wm	$^{16}O_2{}^{13}C\cdot\cdot{}^{16}O_2^-$
1862.4 sh	1862.5 wm		$^{16}O_2{}^{12}C\cdot\cdot{}^{16}O_2^-$
1865.1 wm	1864.6 wm, br		$^{16}O_2{}^{12}C\cdot\cdot{}^{16}O_2^-$
1895.2 vs	1895.2 ms	1895.3 wm	$^{16}O_2{}^{12}C\cdot\cdot{}^{16}O_2^-$
1896.4 sh	1896.2 sh	1896.5 sh	$^{16}O_2{}^{12}C\cdot\cdot{}^{16}O_2^-$

[a] w = weak, m = medium, s = strong, vs = very strong, sh = shoulder, and br = broad.

These absorptions could be separated into groups according to their behavior on filtered photolysis of the sample. Although little change in the absorption pattern resulted from a brief period of irradiation of the sample at wavelengths longer than 490 nm, substitution of the 420-nm cutoff filter resulted in a decrease in the intensities of the absorptions assigned to O_3^-, O_4^+, and O_4^-, consistent with the photolytic behavior previously reported[29] for these species, as well as of the absorptions at 1009, 1430, 1436, 2249, and 3255 cm^{-1}. Similar results were observed when filters with short-wavelength cutoffs near 345, 300, or 280 nm were used. However, when the 260-nm cutoff filter was substituted or no filter was used, the absorptions at 697.1, 1256.5, 1865.1, and 1895.2 cm^{-1} also diminished in intensity, suggesting that they were contributed by a single product species, for which the absorption frequencies are summarized in the first column of Table I. In several of the photolysis studies conducted with the 260-nm cutoff filter or without a filter, there was a slight growth in the 2045.1-cm^{-1} peak.

Isotopic substitution experiments provide additional information about the carrier of the absorptions with a photodecomposition threshold near 260 nm. These absorptions are shown in traces b of Figure 1, and their frequencies are summarized in the second column of Table I, for an experiment conducted using a CO_2 sample enriched to 51.6% in carbon-13. All four of the product

(27) Knight, L. B., Jr.; Steadman, J. *J. Chem. Phys.* **1982**, *77*, 1750.
(28) Knight, L. B., Jr. *Acc. Chem. Res.* **1986**, *19*, 313.
(29) Thompson, W. E.; Jacox, M. E. *J. Chem. Phys.* **1989**, *91*, 3826.
(30) Certain commercial instruments and materials are identified in this paper in order to specify adequately the experimental procedure. In no case does such identification imply recommendation or endorsement by the National Institute of Standards and Technology, nor does it imply that the instruments or materials identified are necessarily the best available for the purpose.
(31) Haugsjaa, P. O. *Rev. Sci. Instrum.* **1986**, *57*, 167.
(32) Jacox, M. E.; Olson, W. B. *J. Chem. Phys.* **1987**, *86*, 3134.
(33) Jacox, M. E.; Milligan, D. E. *J. Mol. Spectrosc.* **1972**, *43*, 148.
(34) Spiker, R. C., Jr.; Andrews, L. *J. Chem. Phys.* **1973**, *59*, 1851.
(35) Milligan, D. E.; Jacox, M. E.; Guillory, W. A. *J. Chem. Phys.* **1970**, *52*, 3864.
(36) Jacox, M. E.; Thompson, W. E. *J. Chem. Phys.* **1990**, *93*, 7609.
(37) Moll, N. G.; Clutter, D. R.; Thompson, W. E. *J. Chem. Phys.* **1966**, *45*, 4469.

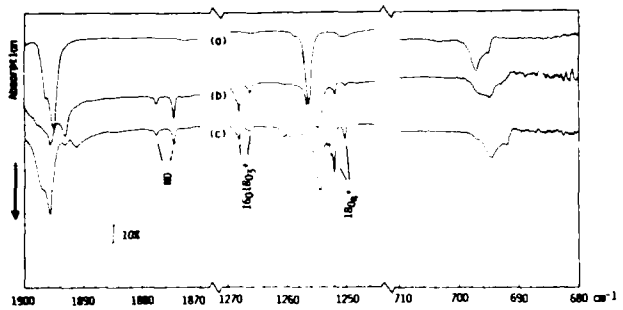

Figure 2. (a) 6.53 mmol of $Ne:CO_2:O_2$ = 200:1:1 codeposited over period of 134 min with 6.27 mmol of discharged Ne. (b) 6.80 mmol of $Ne:CO_2:O_2$ (58.7% ^{18}O) = 200:1:1 codeposited over period of 140 min with 6.07 mmol of discharged Ne. (c) 6.53 mmol of $Ne:CO_2:O_2$ (93% ^{18}O) = 200:1:1 codeposited over period of 205 min with 7.38 mmol of discharged Ne.

absorptions of the unenriched sample were present. The structured absorption at 697.1 cm^{-1} and the more prominent absorption at 1256.5 cm^{-1} each were accompanied by a lower frequency absorption of similar intensity and contour. A relatively sharp, rather prominent absorption of NO_2^- also appeared at 1241.4 cm^{-1}. The 1800–1900-cm^{-1} spectral region was more complicated. In addition to the broad, structured absorption near 1865 cm^{-1} and the prominent 1895.2-cm^{-1} peak, a pair of sharp, moderately intense absorptions of NO appeared in the 1875–1880-cm^{-1} spectral region, a prominent, well-resolved pair of absorptions appeared at 1832.7 and 1835.6 cm^{-1}, and a low-frequency shoulder at about 1861 cm^{-1} appeared on the 1865-cm^{-1} absorption. As is shown in traces c of Figure 1 and in the third column of Table I, the peaks characteristic of experiments with unenriched CO_2 were weak when a $Ne:CO_2$ (90% ^{13}C):O_2 sample was used, and the new peaks of the 51.6% carbon-13 substitution study appeared with enhanced intensity.

Changes were also noted when the isotopic composition of the O_2 in the $Ne:CO_2:O_2$ sample was varied. The absorption patterns in these three spectral regions are compared in traces a, b, and c, respectively, of Figure 2 for an unenriched $Ne:CO_2:O_2$ sample, for a sample prepared by using O_2 with 58.7% random enrichment in oxygen-18, and for a sample prepared by using O_2 with 93% oxygen-18 enrichment. Moderately intense NO absorptions also contributed to the spectra of the two samples prepared with oxygen-18-enriched O_2. Moreover, sharp, structured absorptions of $^{16}O^{18}O_3^+$ and of $^{18}O_4^+$ also appeared between about 1250 and 1270 cm^{-1}. Contour changes occurred for each of the three most prominent absorptions of the product with photodecomposition threshold near 260 nm, and the peaks near 1257 and 697 cm^{-1} shifted to slightly lower frequencies. The absorption frequencies observed for this product in the experiments using O_2 enriched in oxygen-18 are compared with those of the unenriched sample in Table II.

When samples prepared with oxygen-18-enriched O_2 were exposed to unfiltered mercury-arc radiation or to radiation transmitted by the 260-nm cutoff filter for a few minutes, the absorptions summarized in the second and third columns of Table II diminished in intensity, but new, less intense absorptions appeared near them. A more quantitative description of this phenomenon will be presented below.

The three spectral regions of especial interest are shown in Figure 3 for a sample prepared by using CO_2 with 50% random enrichment in oxygen-18, and the absorption frequencies of the species that have a 260-nm photodecomposition threshold are summarized in the first column of Table III. In this experiment, three structured absorptions of similar contour appeared between about 675 and 700 cm^{-1}, with the central absorption approximately twice as intense as the other two. Unfortunately, the experiment was complicated by an exceptionally great concentration of nitrogen oxides produced in the discharge tube, resulting in the appearance of a very prominent NO_2^- absorption at 1241.5 cm^{-1}. However, the 1256-cm^{-1} absorption was accompanied by three new absorptions near 1200, 1228, and 1230 cm^{-1}. Because of the two very strong NO peaks in the 1875–1880-cm^{-1} spectral region, the spectrum between 1850 and 1900 cm^{-1} shown in Figure 3 was obtained by subtracting from the initial spectrum that obtained

TABLE II: Absorptions[a] (cm^{-1}) with a Photodestruction Threshold near 260 nm Observed for $Ne:CO_2:O_2$ = 200:1:1 Samples Prepared with Normal and Oxygen-18-Enriched O_2 and Codeposited at 5 K with a Beam of Excited Neon Atoms

$C^{16}O_2 + {}^{16}O_2$	$C^{16}O_2 + O_2$ (58% ^{18}O)	$C^{16}O_2 + O_2$ (93% ^{18}O)	assignment
		692.1 sh	$^{16}O_2C{\cdot\cdot}{}^{18}O_2^-$
		694.5 m	$^{16}O_2C{\cdot\cdot}{}^{18}O_2^-$
	694.8 m		$^{16}O_2C(^{16}O^{18}O)^-$
695.2 sh			$^{16}O_2C{\cdot\cdot}{}^{16}O_2^-$
	696.4 sh		$^{16}O_2C(^{16}O^{18}O)^-$
697.1 m			$^{16}O_2C{\cdot\cdot}{}^{16}O_2^-$
		1254.5 s	$^{16}O_2C{\cdot\cdot}{}^{18}O_2^-$
	1254.9 ms		$^{16}O_2C(^{16}O^{18}O)^-$
	1255.6 sh		$^{16}O_2C(^{16}O^{18}O)^-$
1256.5 s	1256.2 sh		$^{16}O_2C{\cdot\cdot}{}^{16}O_2^-$
		1844.0 w, br	$^{16}O_2C{\cdot\cdot}{}^{18}O_2^-$
1862.4 sh			$^{16}O_2C{\cdot\cdot}{}^{16}O_2^-$
1865.1 wm			$^{16}O_2C{\cdot\cdot}{}^{16}O_2^-$
		1891.2 wm	$^{16}O_2C{\cdot\cdot}{}^{18}O_2^-$
	1893.2 ms	1893.1 w	$^{16}O_2C(^{16}O^{18}O)^-$
1895.2 vs			$^{16}O_2C{\cdot\cdot}{}^{16}O_2^-$
	1895.6 s	1895.6 vs	$^{16}O_2C{\cdot\cdot}{}^{18}O_2^-$
1896.4 sh			$^{16}O_2C{\cdot\cdot}{}^{16}O_2^-$
		1897.0 sh	$^{16}O_2C{\cdot\cdot}{}^{18}O_2^-$

[a] w = weak, m = medium, s = strong, vs = very strong, sh = shoulder, and br = broad. $C(^{16}O^{18}O)$ indicates that the oxygen isotope of the $^{16}O^{18}O^-$ moiety which is bonded to the carbon atom has not been determined.

TABLE III: Absorptions[a] (cm^{-1}) with a Photodestruction Threshold near 260 nm Observed for an Unphotolyzed $Ne:CO_2$ (50% ^{18}O):O_2 = 200:1:1 Sample, Compared to Absorptions Which Appeared in $Ne:CO_2:O_2$ = 200:1:1 Samples with Mixed Oxygen Isotopic Substitution after Brief Mercury-Arc Irradiation, $\lambda > 260$ nm[b]

CO_2 (50% ^{18}O) + $^{16}O_2$	$C^{16}O_2 + {}^{18}O_2 + h\nu$	$C^{18}O_2 + {}^{16}O_2 + h\nu$	assignment
674.2 w			$^{18}O_2C{\cdot\cdot}{}^{16}O_2^-$
675.7 w			$^{18}O_2C{\cdot\cdot}{}^{16}O_2^-$
	682.3 w, ?		
684.8 wm	684.7 wm	684.2 wm	$^{16}O^{18}OC{\cdot\cdot}{}^{16}O_2^-$
686.3 wm	685.9 wm	685.7 wm	$^{16}O^{18}OC{\cdot\cdot}{}^{16}O_2^-$
	692.1 sh		
	694.5 m		$^{16}O_2C{\cdot\cdot}{}^{18}O_2^-$
695.0 w			$^{16}O_2C{\cdot\cdot}{}^{16}O_2^-$
696.6 w			$^{16}O_2C{\cdot\cdot}{}^{16}O_2^-$
1197.3 w, sh			$^{18}O_2C{\cdot\cdot}{}^{16}O_2^-$
1200.1 w			$^{18}O_2C{\cdot\cdot}{}^{16}O_2^-$
	1226.4 wm	1226.4 wm	$^{16}O''^{18}O''C(^{16}O^{18}O)^-$
	1226.9 wm		
	1227.4 wm		
1228.5 wm	1228.4 wm	1228.4 wm	$^{16}O''^{18}O''C{\cdot\cdot}{}^{16}O_2^-$, $^{18}O''^{16}O''C(^{16}O^{18}O)^-$
	1229.1 sh		
1230.7 wm			$^{18}O''^{16}O''C{\cdot\cdot}{}^{16}O_2^-$
		1254.6 w	$^{16}O_2C{\cdot\cdot}{}^{18}O_2^-$
1256.6 wm			$^{16}O_2C{\cdot\cdot}{}^{16}O_2^-$
1858.0 w			
1862.4 s	1862.5 wm		$^{18}O_2C{\cdot\cdot}{}^{16}O_2^-$
1870.2 m	1870.1 w		$^{18}O_2C{\cdot\cdot}{}^{16}O_2^-$
1871.7 wm, sh			$^{16}O^{18}OC{\cdot\cdot}{}^{16}O_2^-$
	1878.6 m	1878.6 m	$^{16}O^{18}OC(^{16}O^{18}O)^-$
1879.8 sh			$^{16}O^{18}OC{\cdot\cdot}{}^{16}O_2^-$
1880.6 sh			$^{16}O^{18}OC{\cdot\cdot}{}^{16}O_2^-$
1881.8 m	1881.6 w, sh		$^{16}O^{18}OC{\cdot\cdot}{}^{16}O_2^-$
	1882.9 wm	1882.9 wm	$^{16}O^{18}OC(^{16}O^{18}O)^-$
	1884.4 sh	1884.5 sh	$^{16}O^{18}OC(^{16}O^{18}O)^-$
		1893.4 w	$^{16}O_2C{\cdot\cdot}{}^{18}O_2^-$
1895.3 m			$^{16}O_2C{\cdot\cdot}{}^{16}O_2^-$
		1895.7 w	$^{16}O_2C{\cdot\cdot}{}^{18}O_2^-$
1896.5 sh			$^{16}O_2C{\cdot\cdot}{}^{16}O_2^-$

[a] w = weak, m = medium, s = strong, vs = very strong, and sh = shoulder. $C(^{16}O^{18}O)$ indicates that the oxygen isotope of the $^{16}O^{18}O^-$ moiety which is bonded to the carbon atom has not been determined. [b] All samples were codeposited at 5 K with a beam of excited neon atoms.

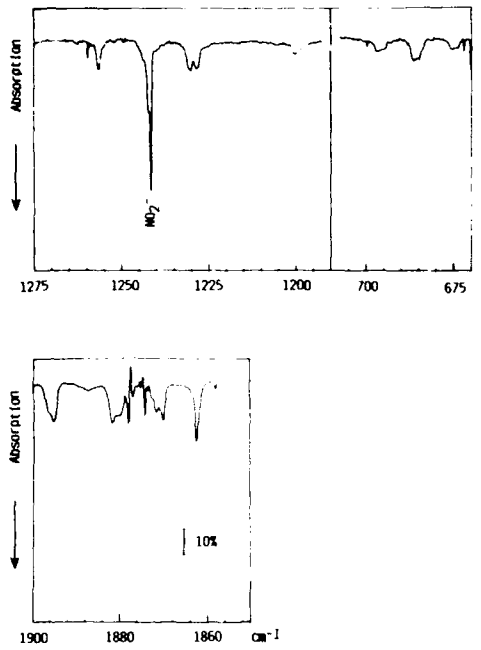

Figure 3. 9.31 mmol of Ne:CO_2 (50% ^{18}O):O_2 = 200:1:1 codeposited over period of 216 min with 9.52 mmol of discharged Ne. For the 1850–1900-cm^{-1} spectral region, spectrum after 30-min mercury-arc photolysis, $\lambda > 260$ nm, was subtracted from spectrum of initial deposit in order to remove very prominent NO impurity absorptions near 1875 and 1880 cm^{-1}.

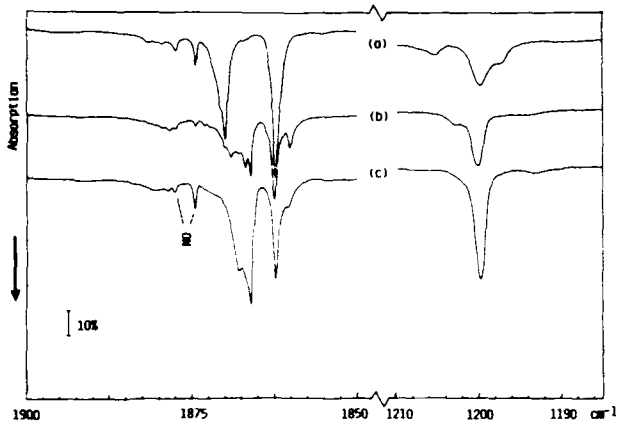

Figure 4. (a) 7.17 mmol of Ne:CO_2 (97% ^{18}O):O_2 = 200:1:1 codeposited over period of 154 min with 6.65 mmol of discharged Ne. (b) 6.56 mmol of Ne:CO_2 (97% ^{18}O):O_2 (58.7% ^{18}O) = 200:1:1 codeposited over period of 160 min with 6.95 mmol of discharged Ne. (c) 7.27 mmol of Ne:CO_2 (97% ^{18}O):O_2 (93% ^{18}O) = 200:1:1 codeposited over period of 186 min with 7.66 mmol of discharged Ne.

after exposing the sample to unfiltered mercury-arc radiation for 30 min, during which the absorptions of the product of interest were completely destroyed. The two sharp peaks with associated negative-going structure resulted from minor contour changes in the two NO peaks. In addition to this extraneous structure, the subtraction spectrum shows four approximately equally spaced product absorptions, each with similar intensity but with a unique contour.

A series of experiments were also conducted using a CO_2 sample enriched to 97% in oxygen-18 and unenriched, 58% randomly oxygen-18 enriched, and 93% oxygen-18 enriched O_2. The 1185–1210- and 1850–1900-cm^{-1} spectral regions of these three experiments are shown in traces a, b, and c of Figure 4, and the positions of the absorptions that were destroyed by radiation near 260 nm are summarized in Table IV. (The detector used for this series of experiments had an exceptionally high signal-to-noise ratio in the mid-infrared region but a sharp cutoff very near 675 cm^{-1}.) The absorptions shown in the first column of Table IV have counterparts among the absorptions for the CO_2 sample with 50% random enrichment in oxygen-18, summarized in the first column of Table III. As for the series of experiments on mixtures that contained $C^{16}O_2$ and O_2 with a varying extent of oxygen-18 enrichment, changes in band contours and relatively small but definite frequency shifts were observed for the samples prepared with $C^{18}O_2$ and with oxygen-18-enriched O_2.

When the Ne:$C^{18}O_2$:$^{16}O_2$ sample of Figure 4a was subjected to a brief period of irradiation with a 260-nm cutoff, new absorptions again appeared near the initially present photolyzable product absorptions. Most of the new peaks corresponded closely with peaks that appeared in the early stages of photolysis of the Ne:$C^{16}O_2$:$^{18}O_2$ sample. The positions and approximate relative intensities of these new absorptions for the Ne:$C^{16}O_2$:$^{18}O_2$ and Ne:$C^{18}O_2$:$^{16}O_2$ samples are summarized in the second and third columns, respectively, of Table III.

In all of the experiments on isotopically substituted samples except that on the Ne:$C^{18}O_2$:$^{18}O_2$ system, weak to moderately intense counterparts of the very sharp, structured 2045.1-cm^{-1} absorption, already tentatively attributed to CO_3, appeared. In Table V, the positions of these absorptions are compared with those reported by Moll et al.[37] for isotopically substituted CO_3. In all of the present mixed oxgyen isotopic experiments, the peak(s) assigned to $^{16}O^{18}OC{=}^{16}O$ or to $^{16}O^{18}OC{=}^{18}O$ were more prominent than those assigned to $^{16}O_2C{=}^{18}O$ or to $^{18}O_2C{=}^{16}O$, as would be expected if CO_3 were to be formed in a process that leads to randomization in the oxygen isotopic distribution. Although the number of peaks and their approximate relative intensities in the studies of isotopically substituted Ne:CO_2:O_2 samples are consistent with the assignment of the 2045.1-cm^{-1} absorption to

TABLE IV: Absorptions[a] (cm^{-1}) with a Photodestruction Threshold near 260 nm Observed for Ne:CO_2 (97% ^{18}O):O_2 = 200:1:1 Samples Prepared with Normal and Oxygen-18-Enriched O_2 and Codeposited at 5 K with a Beam of Excited Neon Atoms

$C^{18}O_2 + {}^{16}O_2$	$C^{18}O_2 + O_2$ (58% ^{18}O)	$C^{18}O_2 + O_2$ (93% ^{18}O)	assignment
1197.4 sh			$^{18}O_2{}^{12}C{\cdot\cdot}{}^{16}O_2^-$
1199.9 ms		1199.8 vs	$^{18}O_2C{\cdot\cdot}O_2^-$
	1200.2 s		$^{18}O_2C{\cdot\cdot}{}^{18}O^{16}O^-$
	1202.7 sh		$^{18}O_2C{\cdot\cdot}{}^{16}O^{18}O^-$
1205.4 wm			$^{18}O_2C{\cdot\cdot}{}^{16}O_2^-$
		1212.8 w	
		1216.0 w	
	1860.2 m	1860.4 sh	$^{18}O_2C(^{16}O^{18}O)^-$
1862.4 vs	1862.5 s	1862.3 s	$^{18}O_2C{\cdot\cdot}O_2^-$
	1866.1 ms	1866.2 vs	$^{18}O_2C{\cdot\cdot}{}^{18}O_2^-$
	1866.9 sh		$^{18}O_2C(^{16}O^{18}O)^-$
	1867.9 sh	1867.9 sh	$^{18}O_2C{\cdot\cdot}{}^{18}O_2^-$
	1869.1 m		$^{18}O_2C(^{16}O^{18}O)^-$
1870.1 s	1870.1 sh		$^{18}O_2C{\cdot\cdot}{}^{16}O_2^-$
	1873.2 sh		$^{18}O_2C(^{16}O^{18}O)^-$
	1874.6 w		$^{18}O_2C(^{16}O^{18}O)^-$
	1877.6 sh		$^{18}O_2C(^{16}O^{18}O)^-$
	1878.5 wm		$^{18}O_2C(^{16}O^{18}O)^-$
	1879.5 sh		$^{18}O_2C(^{16}O^{18}O)^-$

[a] w = weak, m = medium, s = strong, vs = very strong, and sh = shoulder. $C(^{16}O^{18}O)$ indicates that the oxygen isotope of the $^{16}O^{18}O$ moiety which is bonded to the carbon atom has not been determined. When atomic mass of O atom is not designated, absorptions of ^{16}O and ^{18}O species coincide.

TABLE V: Absorptions (cm^{-1}) Assigned to ν_1 of CO_3 in a Neon and a Carbon Dioxide Matrix

species	Ne matrix	CO_2 matrix[a]
$^{16}O_2{}^{12}C{=}^{16}O$	2045.1	2045.3
$^{16}O_2{}^{13}C{=}^{16}O$	1991.2	1990.7
$^{16}O^{18}O^{12}C{=}^{16}O$	2039.0	2039.4
$^{16}O_2{}^{12}C{=}^{18}O$	2022.6	2024.7
$^{18}O_2{}^{12}C{=}^{16}O$	2029.8	2031.4
$^{16}O^{18}O^{12}C{=}^{18}O$	2015.2	2018.3
$^{18}O_2{}^{12}C{=}^{18}O$		2008.0

[a] Reference 37.

CO_3, frequency deviations as great as 3.1 cm^{-1} from the CO_2 matrix values were observed for some of the mixed oxygen isotopic species. These frequency deviations do not preclude assignment of the neon-matrix absorptions to CO_3, since the 2045-cm^{-1} C=O stretching fundamental of CO_3 has been demonstrated[37] to be in strong Fermi resonance with an overtone band near 1880 cm^{-1}. It is quite possible that the matrix shift of the overtone band in a neon matrix differs from that in a CO_2 matrix, implying a pattern of Fermi resonance interaction for the oxygen isotopic species of CO_3 in a neon matrix which differs somewhat from that observed in a CO_2 matrix.

Discussion

The isotopic substitution studies have demonstrated that the species with a photodecomposition threshold near 260 nm (1) possesses a single carbon atom, (2) possesses a CO_2 group, and (3) possesses an O_2 group. The results of the 50% oxygen-18-substituted CO_2 studies also require that the two CO bonds of the CO_2 group be nonequivalent. The complexity of the absorption pattern between 1850 and 1900 cm^{-1} in the experiments on systems with 58.7% randomly oxygen-18-enriched O_2 is sufficiently great to be consistent with a product with two nonequivalent O atoms in the O_2 moiety, but this conclusion is somewhat less firmly established by the infrared data.

The sampling conditions used for these experiments also favor the stabilization of molecular ions. It would be difficult to envision a photodecomposition mechanism for an uncharged $CO_2 \cdot\cdot O_2$ complex in the mid-ultraviolet spectral region, since breaking of the weak bond of the complex would be followed by rapid cage recombination; neither CO_2 nor O_2 could migrate through the rare gas matrix under the conditions of these experiments. Moreover, the presence of the discharge is necessary for the appearance of the new absorptions. Thus, the absorptions of interest are expected to be contributed by either CO_4^+ or CO_4^-. Although molecular anions commonly have a low-energy photodetachment threshold, previous gas-phase studies[22-25] have demonstrated that CO_4^- is stable at least out to 350 nm. Since overall charge neutrality of matrix deposits must be preserved, some Coulombic stabilization of CO_4^- against photodetachment of the electron should also occur in a matrix environment. Beyer and Vanderhoff[38] first reported a gas-phase photodissociation threshold for CO_4^+ near 600 nm. Interestingly, the photodissociation products were CO_2^+ and O_2, rather than the less energetic CO_2 and O_2^+ pair. Similar results were later reported by Smith and co-workers,[39,40] who found that the photodissociation maximum lies near 480 nm. The photodissociation dynamics of this transition have recently been studied by Bowers and co-workers.[6] Because the molecular photodissociation products would be subject to rapid cage recombination in the matrix experiments, net photodissociation of CO_4^+ at wavelengths longer than the 350-nm limit of the gas-phase observations would not occur in neon matrix studies. As for other molecular cations, photodestruction could result from photodetachment of electrons from anions in the system. The relatively mobile electrons thus produced would neutralize cations, resulting in a decrease in their infrared absorptions. Photodestruction of O_4^-, which has a prominent infrared absorption at 973 cm^{-1}, was observed in the present series of experiments, as well as in the earlier Ne:O_2 studies,[29] when the sample was exposed to 420-nm cutoff radiation. The electron flux resulting from photodetachment from O_4^- and from the infrared-inactive O_2^- at this stage of the experiment was sufficiently great to result in complete destruction of O_4^+, yet the absorptions of the new species were unchanged. Their invariance under conditions that should lead to electron capture by CO_4^+ supports the assignment of the absorptions of interest to CO_4^-.

Earlier, unpublished experiments[41] in this laboratory on the infrared spectra of Ar:CO_2:O_2 samples codeposited with a beam of sodium, potassium, or cesium and then subjected to unfiltered mercury-arc irradiation also support the anion identification. As in the corresponding studies[42] on Ar:CO_2 samples codeposited with a beam of an alkali metal, a prominent, complicated pattern of absorptions near 1600 cm^{-1} was contributed by $M^+CO_4^-$. When the sample was subjected to unfiltered mercury-arc radiation, new, weak to moderately intense absorptions appeared at 692, 1259, and 1893 cm^{-1}. In a few of the experiments in which these three peaks were relatively prominent, a weaker absorption also appeared near 1870 cm^{-1}. In a study of an Ar:CO_2 (51.6% ^{13}C):O_2 = 500:2:1 sample codeposited with a beam of potassium atoms, new absorptions appeared at 683, 692, 1250, 1259, 1833, and 1892 cm^{-1} after sample irradiation, also in good correspondence with the product absorptions in the present neon matrix experiments. In the earlier experiments, mercury-arc irradiation would result in photoionization of the alkali metal, and the electron could be captured by CO_2 or by O_2. When O_2 or CO_2 is trapped in an adjacent site in the matrix, reaction to form CO_4^- may follow.

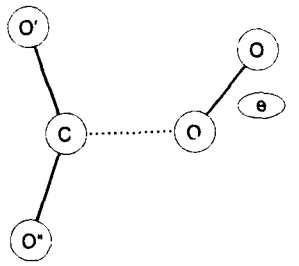

Figure 5. Structure of CO_4^- calculated by ref 19. $R(CO') = R(CO'') = 1.27$ Å; $R(C\cdot\cdot O) = 1.48$ Å; $R(OO) = 1.21$ Å; $\angle(O'CO'') = 140°$; $\angle(C\cdot\cdot OO) = 130°$.

A more detailed analysis of the infrared absorptions observed for CO_4^- requires knowledge of the approximate structure of this species. Ben Taarit and co-workers[19] performed a CNDO/SP calculation of the structure of CO_4^- in the gas phase which they and later workers[20,21] found to give a moderately good fit to the spin densities derived from the studies of the ESR spectrum of CO_4^- on surfaces maintained at 77 K. This structure is shown in Figure 5. Although there have been no more recent calculations of the structure of CO_4^-, similar ion–quadrupole bonding has been studied by Hiraoka and co-workers[43,44] for $O_2C\cdot\cdot Cl^-$ and $O_2C\cdot\cdot F^-$, using both mass spectrometric measurements and ab initio calculations with geometry optimization at the 4-31G level. These workers found the bonding of successive CO_2 units to Cl^- to be exothermic by 6 or 7 kcal/mol. The complex was essentially electrostatic, with coordination between Cl^- and the C atom of each CO_2 unit. The CO_2 groups were only slightly bent. In contrast, they observed the reaction of F^- with CO_2 to be exothermic by 32 kcal/mol. Once again, the halide ion attacked the carbon atom, but in this system there was substantial charge transfer to the CO_2 moiety, and the OCO valence angle decreased to 137.6°. $O_2C\cdot\cdot O_2^-$, with a binding energy of approximately 21 kcal/mol, might be expected to have a structure and chemical bonding properties intermediate between those of the chloride and fluoride complexes. Thus, the structure of Figure 5 appears to provide a reasonable model for further analysis of the infrared spectrum of CO_4^-.

The structure of CO_4^- given in Figure 5, which belongs to the C_s point group, would have seven in-plane vibrations and two out-of-plane vibrations. Because of the relatively weak C··O bond, the two out-of-plane modes, an "umbrella" deformation of the $O_2C\cdot\cdot O$ group and a torsional vibration, should appear at very low frequencies. These experiments give no information regarding them. Therefore, the analysis was confined to the in-plane vibrations. Of these, the three vibrations associated with the CO_2 moiety and the stretching vibration of the O_2^- moiety lie in the mid-infrared region. The C··O stretching vibration and the OC··O

(38) Beyer, R. A.; Vanderhoff, J. A. *J. Chem. Phys.* **1976**, *65*, 2313.
(39) Smith, G. P.; Cosby, P. C.; Moseley, J. T. *J. Chem. Phys.* **1977**, *67*, 3818.
(40) Smith, G. P.; Lee, L. C. *J. Chem. Phys.* **1978**, *69*, 5393.
(41) Jacox, M. E.; Milligan, D. E. Unpublished results.
(42) Jacox, M. E.; Milligan, D. E. *Chem. Phys. Lett.* **1974**, *28*, 163.
(43) Hiraoka, K.; Shoda, T.; Morise, K.; Yamabe, S.; Kawai, E.; Hirao, K. *J. Chem. Phys.* **1986**, *84*, 2091.
(44) Hiraoka, K.; Mizuse, S.; Yamabe, S. *J. Chem. Phys.* **1987**, *87*, 3647

TABLE VI: Comparison of Observed and Calculated[a] Fundamentals (cm^{-1}) of Isotopically Substituted $O_2C{\cdot\cdot}O_2^-$

	ν_1		ν_2		ν_4	
species	obs	calc	obs	calc	obs	calc
$^{16}O_2{}^{12}C{\cdot\cdot}{}^{16}O_2^-$	1895.2	1893.3	1256.5	1253.8	697.1	696.9
$^{16}O_2{}^{13}C{\cdot\cdot}{}^{16}O_2^-$	1832.8	1840.9	1247.6	1238.5	686.4	683.6
$^{16}O'{}^{18}O''{}^{12}C{\cdot\cdot}{}^{16}O_2^-$	1881.8[b]	1878.6	1228.4[b]	1228.5	686.0[b]	688.6
$^{18}O'{}^{16}O''{}^{12}C{\cdot\cdot}{}^{16}O_2^-$	1881.8[b]	1878.2	1230.6[b]	1230.3	686.0[b]	687.7
$^{18}O_2{}^{12}C{\cdot\cdot}{}^{16}O_2^-$	1862.4	1862.4	1199.9	1206.3	675.7	679.0
$^{16}O_2{}^{12}C{\cdot\cdot}{}^{16}O^{18}O^-$		1893.3		1253.8		696.4
$^{16}O_2{}^{12}C{\cdot\cdot}{}^{18}O^{16}O^-$		1893.3		1253.7		693.8
$^{16}O_2{}^{12}C{\cdot\cdot}{}^{18}O_2^-$	1895.6	1893.3	1254.5	1253.7	694.5	693.4
$^{18}O_2{}^{12}C{\cdot\cdot}{}^{16}O^{18}O^-$		1862.4		1206.1		678.5
$^{18}O_2{}^{12}C{\cdot\cdot}{}^{18}O^{16}O^-$		1862.4		1206.0		675.7
$^{18}O_2{}^{12}C{\cdot\cdot}{}^{18}O_2^-$	1866.2	1862.4	1199.8	1205.9		675.2

[a] $F(CO') = F(CO'') = 10.59$, $F(C{\cdot\cdot}O) = 1.27$, $F(CO'CO'') = 0.65$, $F(CO',C{\cdot\cdot}O) = 0.30$, $F(CO'',C{\cdot\cdot}O) = 0.32$, in units of 10^2 N m^{-1}; $F(CO',O'CO'') = 0.21$, $F(CO'',O'CO'') = 0.23$, in units of 10^{-8} N; $F(O'CO'') = 0.89$, $F(O'C{\cdot\cdot}O) = -0.02$, $F(O''C{\cdot\cdot}O) = 0.42$, $F(C{\cdot\cdot}OO) = 0.15$, in units of 10^{-18} N m. $F(OO)$ fixed at 6.0×10^2 N m^{-1}. [b] Not used in the fit.

and C··OO deformation vibrations are expected to lie in the far-infrared region.

The band contour of the 1895-cm^{-1} absorption, which must be assigned to the O=C=O antisymmetric stretching vibration of CO_4^-, ν_1, varies considerably on isotopic substitution. The presence of the weaker absorption near 1865 cm^{-1} suggests that this variation is a consequence of the perturbation of ν_1 by an overtone or a combination band. The frequency sum of the two other observed infrared absorptions of $^{12}C^{16}O_4^-$ is 1953.6 cm^{-1}. Unless the combination of these two fundamentals is highly anharmonic (a possibility for a weakly bonded complex), Fermi resonance interaction between ν_1 and this combination band of CO_4^- would result in the appearance of an absorption near 1950 cm^{-1}. No absorption was observed near this position. Another possible perturbing energy level would be $\nu_3 + \nu_4$, the combination of the OO stretching vibration with the 697.1-cm^{-1} fundamental, which is in the spectral region appropriate for the in-plane OCO bending vibration. The electron spin resonance observations[19-21] suggest that the bonding of CO_4^- results principally from an ion–quadrupole interaction, with relatively little charge transfer from the O_2^- moiety. The ground-state vibrational fundamental of gas-phase O_2^- lies near 1090 cm^{-1}, while that for O_2 is near 1555 cm^{-1}.[45] A small extent of charge transfer from the O_2^- moiety to CO_2 would, therefore, be expected to result in a small increase in the OO stretching frequency. If this frequency were to be near 1170 cm^{-1} in CO_4^-, $\nu_3 + \nu_4$ would lie near 1870 cm^{-1}, an appropriate position for the perturbing energy level. Other possibilities for this energy level may arise from ternary combinations of either the CO_2 symmetric stretching vibration or the OO stretching vibration with an overtone of one of the lower frequency fundamentals or a combination of two of them.

Further analysis of the isotopic data for the in-plane vibrations of CO_4^- was conducted using the least-squares force constant adjustment program FADJ, developed by Schachtschneider.[46] The CNDO/SP structure for CO_4^-, shown in Figure 5, was assumed. Data were insufficient to permit correction for the perturbation of the 1895-cm^{-1} fundamental. The fit to the three observed fundamentals, which correspond to the three in-plane vibrations of the CO_4 moiety, is similar for a variety of different initial force constant sets. An average error of approximately 3 cm^{-1} is typical. The calculated carbon-13 isotopic shift is always about 10 cm^{-1} smaller than the observed shift, a consequence of the uncorrected perturbation of this fundamental by a combination band that lies below ν_1 of $O_2{}^{12}C{\cdot\cdot}O_2^-$ but above ν_1 of $O_2{}^{13}C{\cdot\cdot}O_2^-$. Trial calculations were done for the OO stretching force constant, $F(OO)$, fixed at 6.0×10^2 N m^{-1}, slightly greater than the 5.44×10^2 value for O_2^-, and for $F(OO)$ fixed at 8.4×10^2 N m^{-1}, the mean of the values[29] for O_2 and O_2^-. The calculated frequencies for the CO_2 moiety were almost independent of the value of $F(OO)$. In consideration of the results of the ESR studies, $F(OO)$ was fixed at 6.0×10^2 N m^{-1} for the subsequent calculations. In order to reproduce the observed nonequivalence of the two C=O bonds, which results in the detection of four rather than of three peaks for each of the C=O stretching fundamentals in the observations made using 50% randomly oxygen-18-enriched CO_2, it was necessary to include the O=C··O and C··OO bending force constants, as well as the C··O stretching force constant, in the adjustment.

The results of the final force constant adjustment calculation are summarized in Table VI. All of the diagonal force constants were adjusted except $F(OO)$, which was fixed at 6.0×10^2 N m^{-1}. The two C=O stretching force constants, $F(CO')$ and $F(CO'')$, and the two OC··O bending force constants, $F(O'C{\cdot\cdot}O)$ and $F(O''C{\cdot\cdot}O)$, were individually adjusted, in order to provide for the observed nonequivalence of the two C=O bonds. Three stretching interaction force constants, $F(CO',CO'')$, $F(CO',C{\cdot\cdot}O)$, and $F(CO'',C{\cdot\cdot}O)$, were included, as were two stretch–bend interaction force constants, $F(CO',O'CO'')$ and $F(CO'',O'CO'')$. The calculations predict the observed splitting of approximately 2 cm^{-1} between the CO_2 "symmetric" stretching absorptions (ν_2) of the two species that possess a $^{16}OC^{18}O$ group. They also correctly predict only a small difference between the CO_2 bending frequencies (ν_4) of these two isotopic species, with a value near the mean of the values for species that possess $^{12}C^{16}O_2$ and $^{12}C^{18}O_2$ groups. Only a small shift is calculated on substitution of $^{18}O_2^-$ for the $^{16}O_2^-$ moiety. Although the observed shift is small, its magnitude is underestimated by the calculations. The calculated position of the OO stretching fundamental of $^{16}O_2{}^{12}C{\cdot\cdot}{}^{16}O_2^-$, strongly dependent on the assumed value of $F(OO)$, is 1146 cm^{-1}, the calculated position of the C··O stretching fundamental is 346 cm^{-1}, and the calculated positions of the two low-frequency in-plane deformation modes are 228 and 115 cm^{-1}. Because the information on the three low-frequency modes is indirect, resulting from an adjustment of the force constants that govern them in order to fit the isotopic data for higher frequency vibrational modes, there is a large uncertainty in this estimate of their positions.

Several factors contribute to the relatively large average error, 3.5 cm^{-1}, in the force constant adjustment calculation summarized in Table VI. The perturbation of ν_1 by a nearby combination band has already been discussed. The use of an approximate structure for CO_4^- is also important. Although the calculation is insensitive to the magnitude of bond lengths, it is sensitive to the values chosen for bond angles.

The values obtained for the force constants of CO_4^-, summarized in a footnote to Table VI, provide additional information about the chemical bonding properties of this species. The asymmetry of the two C=O bonds is sufficiently small that $F(CO')$ and $F(CO'')$ are equal to two decimal places. Their value, 10.59×10^2 N m^{-1}, is slightly below the range $((11.8\text{–}13.4) \times 10^2)$ typical of the C=O bond.[47] Even with an assumed value

(45) Huber, K. P.; Herzberg, G. *Molecular Spectra and Molecular Structure. IV. Constants of Diatomic Molecules*; Van Nostrand Reinhold: New York, 1979.

(46) Schachtschneider, J. H. Technical Report Nos. 231-64 and 57-65; Shell Development Co.: Emeryville, CA, 1964; private communication.

(47) Wilson, E. B., Jr.; Decius, J. C.; Cross, P. C. *Molecular Vibrations*; McGraw-Hill: New York, 1955; p 175.

of 8.4×10^2 N m^{-1} for F(OO), the calculated value of the C=O stretching force constants is virtually unchanged. The C=O stretching force constant is significantly larger than that calculated for CO_2^-, 7.92×10^2 N m^{-1}. (This value was inadvertently omitted from Table III of the paper[26] reporting the spectrum of CO_2^- in solid neon.) The large difference between the C=O stretching force constants of CO_2^- and CO_4^- supports the retention of most of the negative charge by the O_2 moiety of CO_4^-. The small negative value found for F(O'C··O) is an artifact resulting from the omission of the F(O'C··O,O''C··O) bending interaction force constant from the calculation. The dissociation energy of the C–O bond of a number of alkyl ethers is approximately 82 kcal/mol,[48] and typical C–O stretching force constants lie in the (5.0–5.8) $\times 10^2$ N m^{-1} range.[47] The ratio of the binding energy of CO_4^-, 21 kcal/mol,[5] to the energy of a C–O bond, assuming such bonds in alkyl ethers to be typical, equals 0.26. If proportionality between the CO bond order and the CO stretching force constant is assumed, F(C··O) should lie between 1.3×10^2 and 1.5×10^2 N m^{-1}, in very good agreement with the value obtained in the force constant adjustment calculation. However, it must be noted that the interaction of O_2^- with CO_2 is accompanied by an electron redistribution in the CO_2 moiety, evidenced by a decrease in the OCO angle. Therefore, the binding energy of $O_2C··O_2^-$ cannot rigorously be considered to be localized in the C··O bond.

As is indicated in Table III, it is possible to assign the absorptions that appear after a brief period of 260-nm cutoff irradiation of $Ne:C^{16}O_2:^{18}O_2$ or $Ne:C^{18}O_2:^{16}O_2$ samples to CO_4^- species for which isotopic randomization has occurred. The frequency of each of the two components of ν_2 of $^{16}O^{18}OC··^{16}O_2^-$ is lowered by about 2 cm^{-1} when $^{16}O^{18}O^-$ is substituted for $^{16}O_2^-$, also supporting the nonequivalence of the two C=O bonds. The isotopic randomization suggests that near 260 nm CO_4^- photodecomposes into CO_3^- (D_{3h}) and O, or into an excited state of CO_3 that has a 3-fold symmetry axis and O^-, followed by cage recombination of the photofragments. Some of the O or O^- formed by this process would diffuse from the site of its photoproduction, resulting in the observed increase in the concentration of CO_3, which could be formed either directly or by electron photodetachment from CO_3^-.

The failure to identify absorptions of CO_4^+ in these experiments may be a consequence of relatively small absorption coefficients or of a low concentration because of competing chemical reactions. Bowers and co-workers[49] found that the rate of charge exchange of CO_2^+ with O_2 is an order of magnitude slower than that of O_2^+ with O_2, implying that the rate of formation of CO_4^+ from $CO_2^+ + O_2$ is relatively slow. The rate of the reaction of O_2^+ with CO_2 with helium as a third body is half that of the corresponding reaction of CO_2 with O_2^-.[4] Because of the rapidity of the $O_2^+ + O_2$ reaction, these comparative rates suggest that most of the O_2^+ may be scavenged by O_2 before it can react with CO_2.

Conclusions

The three fundamental vibrations of CO_2 complexed to O_2^- have been observed at 697, 1256, and 1895 cm^{-1}. Analysis of the infrared absorption pattern of the isotopically substituted CO_4^- products is consistent with a planar $O_2C··O_2^-$ structure in which the O_2C and $C··O_2^-$ groups are bent and the CO bonds of the CO_2 moiety are significantly weaker than those in uncomplexed CO_2. This analysis is insensitive to the vibrational frequency of the O_2^- moiety. The photodestruction threshold of CO_4^- lies near 260 nm. The observation of isotopic randomization of CO_4^- on irradiation at wavelengths near 260 nm suggests that a 3-fold symmetric electronic state of CO_3 or of CO_3^- is one of the photodissociation products.

Acknowledgment. The design and construction of the transfer optics used with the Bomem interferometer and the maintenance of this instrument by Dr. W. Bruce Olson are gratefully acknowledged, as are helpful conversations with Dr. Morris Krauss. This work was supported in part by the U.S. Army Research Office under Research Proposal No. 25664-CH.

Registry No. CO_2, 124-38-9; O_2, 7782-44-7; Ne, 7440-01-9; CO_4^-, 12127-41-2; O_4^-, 12596-84-8; O_4^+, 12596-85-9; ^{18}O, 14797-71-8.

(48) Benson, S. W. *Thermochemical Kinetics*, 2nd ed.; Wiley: New York, 1976; p 309.

(49) Derai, R.; Kemper, P. R.; Bowers, M. T. *J. Chem. Phys.* **1985**, *82*, 4517.